

# OCENA DELOVANJA ENO IN DVOFREKVENČNIH NIZKOCENOVNIH SPREJE- MNIKOV GNSS V STATIČNEM RELATIVNEM NAČINU

# PERFORMANCE EVALUATION OF SINGLE AND DOUBLE- FREQUENCY LOW-COST GNSS RECEIVERS IN STATIC RELATIVE MODE

*Naccieli Bojorquez-Pacheco, Rosendo Romero-Andrade, Manuel Edwiges Trejo-Soto, Daniel Hernández-Andrade, Karan Nayak, Ana Isela Vidal-Vega, Anibal Israel Arana-Medina, Gopal Sharma, Luis Enrique Acosta-Gonzalez, Richard Serrano-Agila*

UDK: 528.28:528.3:528.5  
Klasifikacija prispevka po COBISS.SI: 1.04  
Prispelo: 20. 8. 2022  
Sprejeto: 30. 5. 2023

DOI:10.15292/geodetski-vestnik.2023.02.235-248  
PROFESSIONAL ARTICLE  
Received: 20. 8. 2022  
Accepted: 30. 5. 2023

## IZVLEČEK

Z napredkom nizkocenovnih sprejemnikov GNSS z vgrajenimi sodobnimi zmogljivostmi se je odprlo še eno okno za raziskovanje učinkovitosti različnih nizkocenovnih sprejemnikov s pregledi njihove zmogljivosti in primernosti za različne geodetske namene. Glavni cilj te študije je oceniti učinkovitost določanja položaja eno- in dvofrekvenčnih sprejemnikov GNSS v kombinaciji z geodetskimi antenami v statičnem relativnem načinu glede na mehiške predpise. Zabeležena opazovanja so bila obdelana s statično relativno metodo z navezavo na permanentno postajo mehiškega nacionalnega inštituta za statistiko in geografijo INEGI. Rezultati raziskave, izvedene na razdalji 4 in 33 kilometrov od permanentne postaje, kažejo podobno natančnost za vse nizkocenovne sprejemnike. Za nizkocenovne sprejemnike GNSS NEO-M8T, NEO-6T in ZED-F9P so dobljene rešitve dosegle milimetrске horizontalne natančnosti z uporabo geodetske antene. Z modelom ZED-F9P je mogoče doseči visoko natančnost na večjih oddaljenostih od permanentne postaje. Pri vertikalni komponenti pa se pokaže, da je v vseh primerih slabša kot pri uporabi geodetskih sprejemnikov. Če se ne zahteva višja natančnost od petih centimetrov, lahko uporabimo tudi nizkocenovne sprejemnike GNSS.

## KLJUČNE BESEDE

statična relativna metoda, GNSS, nizkocenovni sprejemniki

## ABSTRACT

The advancement of low-cost GNSS receivers with modern built-up characteristics has opened a new window to investigate the performance of various low-cost receivers with an outlook on their performance and suitability for varied geodetic purposes. The main objective of this study is to evaluate the positioning performance of single and double-frequency GNSS receivers in combination with geodetic antennas in static relative mode regarding Mexican regulations. The recorded observations were processed by a static relative method including the CORS station from the National Institute of Statistics and Geography in Mexico (INEGI). The results of the survey conducted at a distance of 4 and 33 km from CORS station show similar accuracy for all low-cost receivers. For low-cost GNSS receivers NEO-M8T, NEO-6T, and ZED-F9P the solutions that were obtained reached mm in horizontal precision using a geodetic grade antenna. Similarly, the ZED-F9P model was proved at a long distance from the CORS station and presents high precision. Regarding the vertical component, in all cases where the GGM10 model was included, the vertical component is not allowed to use for topography or geodetic works, however, the horizontal component where mm precision was achieved is allowed for different highly precision survey works.

## KEY WORDS

static relative method; GNSS; low-cost receivers

## 1 INTRODUCTION

Nowadays with the constant development of the Global Navigation Satellite System (GNSS), new receivers with compelling characteristics were developed and various studies were conducted using these technologies. During the 90's, the world of Geodesy was introduced to "low-cost GNSS" receivers which are also known as "high sensitivity" receivers due to their capability of tracking -160 dB (Tsakiri et al., 2018) with only a single frequency. In the beginning, these receivers were only used for mapping or Geographic Information Systems (GIS) applications since reaching m level (Tsakiri et al., 2018). Sioulis et al. (2015) test and evaluate the positioning performance of high-sensitivity carrier phase-based navigation receivers based on the official international standards organization (ISO) specifications for real-time kinematic (RTK) GNSS geodetic receivers. The results demonstrate the suitability of the u-blox NEO-7P XXL bundle package with the NEO-7P module for different accuracy levels of RTK positioning applications. Similarly, in the state-of-art, the improvement of the low-cost GNSS receivers is seen in the different research that was conducted. Studies such as sampling rates impact were Precise Point Positioning in static mode showed high accuracy reaching a cm level (Romero-Andrade et al., 2021), the accuracy achievable in the positioning due to the urban areas where the signal is hard to track due the urban canyons reached cm in static relative method, nevertheless, for the vertical component exceeded the reference values from Mexican regulations (Janos & Kuras, 2021; Romero-Andrade et al., 2021). In the case of RTK method, Garrido-Carretero et al. (2019) presented an evaluation of RTK method under ISO-17123-8 as a feasible option in geomatics, they show combined uncertainties as close to  $\pm 5.5$  mm for the horizontal component and  $\pm 11$  mm for heights being useful for high precision applications. Wielgocka et al. (2021) presented the feasibility of using low-cost dual-frequency GNSS receivers for land surveying, they also used a well-known ZED-F9P receiver in conjunction with ANN-MB-00-00 antenna where the obtained results reached cm of precision in PPP with a 2.4 h of the session, regarding the vertical component the results still are inaccurate. As per the Static relative method in short and long distances, Romero-Andrade et al. (2020) and Zamora-Maciel et al. (2020), evaluate a geodetic baseline at  $\sim 5$  and  $\sim 33$  km from the CORS reference station, achieving a mm precision in consideration of survey time. Romero-Andrade et al. (2019) present the reliability of the RTKLib (Takasu, 2013) software used in different embedded systems, also they found that the Precise Point Positioning could be considered for use in different embedded systems and achieve high precision. Cina & Piras (2015), presented the performance of a mass-market GNSS receiver to verify if any such type of sensors could be used for landside monitoring. As per the obtained results some low-cost single frequency GNSS receivers could be possibly considered if the time of acquisition, baseline length, and the antenna is suitable. More recent studies with a clear advance in the state-of-art of crustal deformation studies using GNSS is presented by Tunini et al. (2022), where the applicability of low-cost GNSS receiver is suitable for crustal deformation studies, showing that mm-order precision can be achieved by low-cost GNSS receivers, while the results in terms of time series are largely comparable to those obtained using high-price geodetic receivers. Krietemeyer et al. (2022), propose a new method for antenna calibration that fully relies on low-cost solutions. The proposed method reduces the median deviations of the low-cost antennas in the vertical direction using Post Processed Kinematic (PPK) by 20-24%, also the accuracy reached from 5.6 to 3.8 mm being comparable to geodetic grade antenna. In the same way, the use of smartphones for survey are getting more popular, although, it is out of this contribution, some examples are given (Läpädat et al., 2021; Psychas et al., 2019; Skorupa, 2020). Notti et al.

(2020) prove the potentiality of low-cost GNSS continuous monitoring applied to an unstable slope, also it proposes a new methodological approach that considers the use of semi-automatized procedures for the identification of anomalous trends and a risk communication strategy. Hamza et al. (2020), determined the positional precision within static survey, and displacement detection within dynamic survey using a ZED-F9P and u-blox ANN-MB-00 antenna, it was stated that it can detect displacements from 10 mm upwards with a high level of reliability. Hamza et al. (2021) demonstrated the suitability of the ZED-F9P low-cost GNSS receiver and calibrated low-cost antennas for different geodetic applications. Their result was compared with a geodetic GNSS instrument, showing that variations were up to 1 mm difference in horizontal and vertical components of less than 0.6 mm. Similarly, Janos & Kuras (2021) evaluated the accuracy of a position determination using low-cost receivers in different terrain conditions, in most of the cases, the partially obscured horizon obtained a high precision position using a low-cost GNSS receiver ZED-F9P. Manzini et al. (2020) used a low-cost GNSS receiver for structural health monitoring (SHM), using a combination of different antennas and receivers. It was proved that it is possible to track quick displacements down to 4 mm and oscillations of 1 cm with a frequency up to 0.254 hz with 1 hz receiver. The conclusion was that the low-cost GNSS showed a good agreement between GNSS time series and traditional displacement sensor, and numerical simulations made using an operational mechanical model of the bridge. Poluzzi et al. (2019) utilized the low-cost GNSS receivers for monitoring applications with an aim to assess on one hand the capability of the systems to perform the monitoring of slow displacements with the best possible precision, and on the other hand, the performances of the real-time solutions that can be used for early warning purposes. The precisions evidenced by the test shows such low-cost instrumentations can be used for many applications monitors purposes. Xue et al. (2022) analyzed the performance of low-cost GNSS receivers in monitoring dynamic motion using a closely-spaced dual low-cost GNSS receiver's system to enhance their performance. It was shown that the precision of the low-cost GNSS receivers could be enhanced to the level of 2-4 mm, by using multi-GNSS observations and limiting the noise level based on error modeling and filtering on the closely-spaced low-cost GNSS receivers. Also, it was proved that the low-cost GNSS receivers could accurately define modal frequencies of  $-0.362$  hz and  $-1.680$  hz, respectively.

Based on this, the main research is focusing on the use of the real time techniques for monitoring, but at this point is important for the engineers to solve the topographic-geodetic problems with the implementation of different alternatives for the geodetic grade receivers that are expensive (a low-cost GNSS receivers cost  $\sim 300\text{€}$ , that represents  $\sim 80\%$  less than a geodetic receiver). With regards to the processing method, the static relative method is the most precise technique to obtain a high accuracy and precision (Hofmann-Wellenhof et al., 2001). The GNSS observations processing software commonly uses the Static relative method to obtain high precision of positioning. Nevertheless, the Static relative method has the main disadvantage of the observation and the dependence of the reference station with known coordinates (Romero-andrade et al., 2021). The collected data could be processed with topographic or scientist software with dependence to the objective of the job (for topographic purposes is commonly used a commercial software) (Ferhat et al., 2015). Based on this fact, the main objective of this research is to compare the performance and suitability in the positioning precision using different low-cost receivers in static relative method with geodetic grade antenna on pillars located at a distance of  $\sim 5$  and  $\sim 33$  km from the reference station.

## 2 TEST AREA

Two cases were taken into consideration, case A and B, where the case A is situated ~5 km from the reference station at the roof of the Faculty of Earth and Space Sciences (Figure 1) and case B is ~33 km from the reference station at Sanalona village (Figure 2) that belongs to Culiacan City in Mexico. In both cases the antenna was collocated with a clean surrounding antenna environment and optimal weather conditions. In the first case, Case A, 3 pillars were selected to avoid the centering problem, and for the Case B, 2 pillars were used in the village of Sanalona. All locations were measured with geodetic order receiver at the same time and day with an aim to maintain similar conditions for the low-cost GNSS receivers.

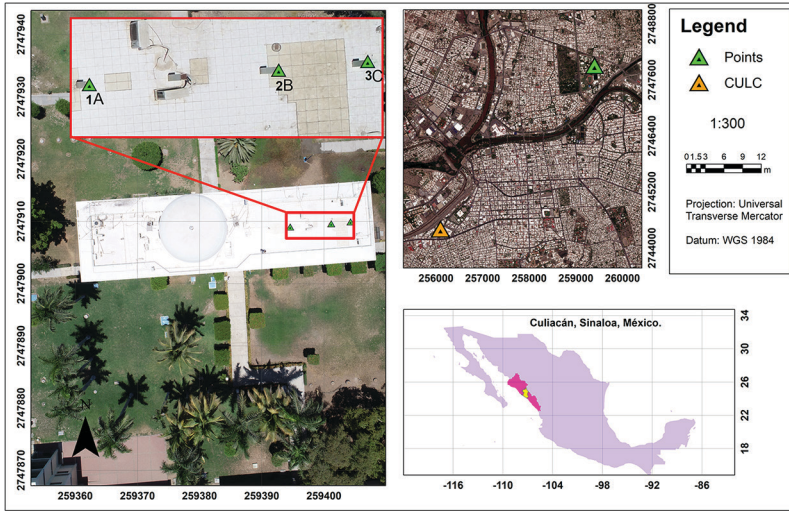


Figure 1: Case A: Pillars located on the roof of the Earth and Space Sciences faculty building, with clean surrounding antenna environment and optimal weather condition at ~5 km from Reference station.

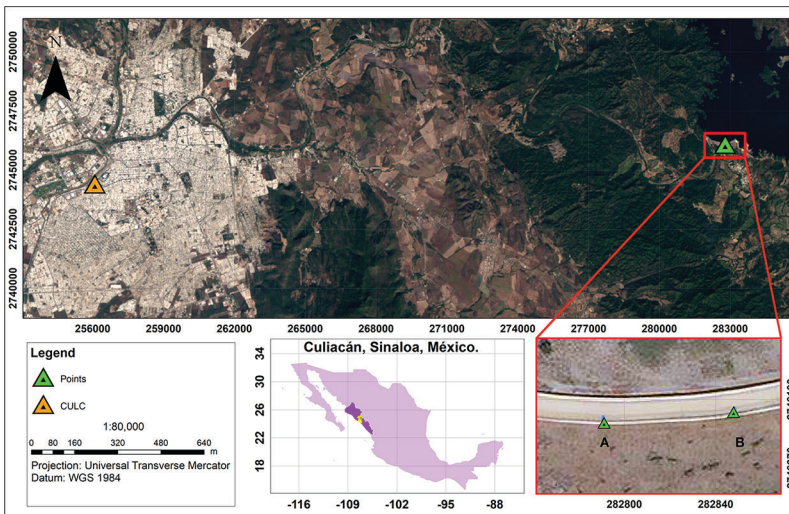


Figure 2: Case B: Pillars located in the village of Sanalona at 33 km of distance from the Reference station.



3 METHODOLOGY

3.1 GNSS data collection and processing

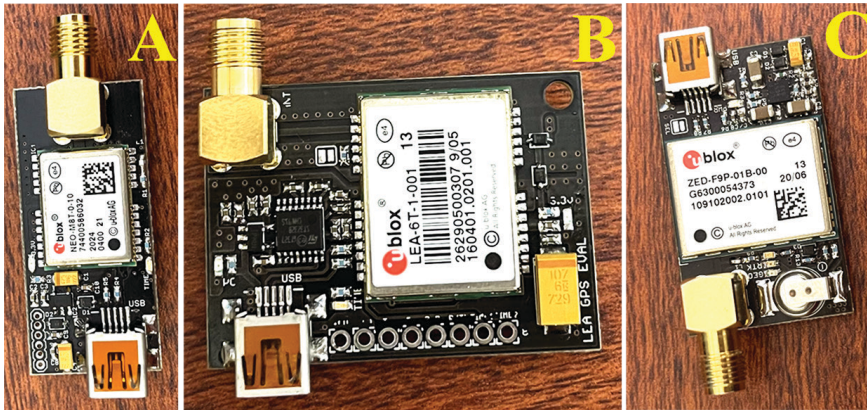


Figure 3: Low-cost GNSS receivers: (a) NEO-M8T; (b) LEA-6T; (c) ZED-F9P



Figure 4: Antennas and stations used for the experiment. A) CULC CORS station from INEGI. B) GEOMAX ZENITH25. C) ASH701975.01A

Three different low-cost GNSS receivers (ZED-F9P, NEO-M8T, and LEA-6T) of the u-blox series were used for acquiring the observations with Geodetic Antenna (ASH701975.01A) (Figure 3-4 and Table 1) where the main characteristics of all receivers have the capability to track GPS signals at high or low frequencies. With the purpose of testing the accuracy of the low-cost devices using static relative method, ZED-F9P model was used in the village of Sanalona since it is a dual-frequency GNSS receiver and according to the state-of-art is the most stable receiver. The low-cost receiver is situated at a distance of ~33 km from the reference station CULC belonging to the INEGI (National Institute of Statistics and Geography, <https://www.inegi.org.mx/app/geo2/rgna/>) geodetic network. The obtained coordinates from geodetic GNSS receiver were taken as a reference for comparison purposes since in a normal geodetic-topographic work it is commonly used to obtaining solutions from geodetic order GNSS receivers.

Table 1: Characteristics of the low-cost receivers used for the experiment (these characteristics are from receiver and not based in the applied technique).

| Receiver type  | Convergence time                              | Sensitivity                                                                                        | Supported signal                                                                                   |
|----------------|-----------------------------------------------|----------------------------------------------------------------------------------------------------|----------------------------------------------------------------------------------------------------|
| <b>LEA-M8T</b> | Cold starts: 25 s;<br>aided cold starts: 2 s. | Tracking and Nav: -167 to -166 dBm; Cold start: -157 to -157 dBm; Reacquisition: -160 to -160 dBm. | GPS/QZSS L1 C/A, GLONASS L10F, BeiDou B1<br>SBAS L1 C/A: WAAS, EGNOS, MSAS, GAGAN<br>Galileo E1B/C |
| <b>ZED-F9P</b> | RTK < 10 s                                    | Tracking & Nav. -167 dBm; Cold starts -148 dBm; Hot starts -157 dBm; Reacquisition -160 dBm        | GPS L1C/A L2C, GLO L1OF L2OF,<br>GAL E1B/C E5b, BDS B1I B2I, QZSS L1C/A L1S L2C, SBAS L1C/A        |
| <b>NEO-6T</b>  | Cold starts: 26 s;<br>hot starts: 1 s         | Tracking: -162 dBm; Cold starts: -148 dBm; Hot starts: -157 dBm                                    | GPS L1 C/A code<br>SBAS: WAAS, EGNOS, MSAS                                                         |

The methodology applied for this research is presented in Figure 5.

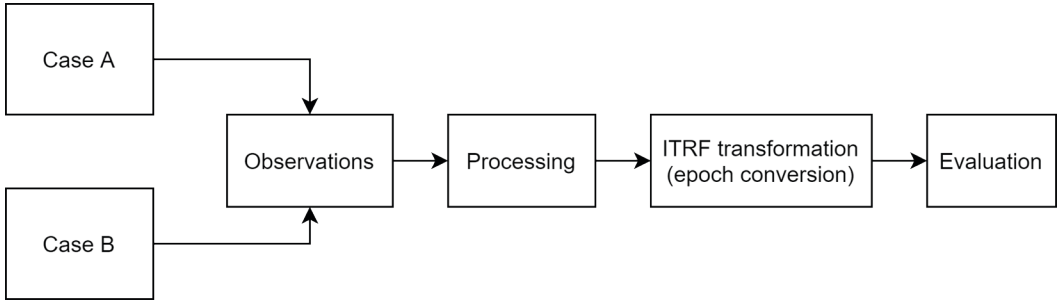


Figure 5: Flowchart of the methodology implemented in the research.

All the low-cost GNSS receivers were controlled using a Laptop with U-Center (Ublox, 2022) software, for which the receivers provide the data in a binary format “ubx”, which are then converted using RTKLIB (Takasu, 2013) software to RINEX (Gurtner, 1994) format, securing the data in the system. The elimination of the constellations was carried out using TEQC software (Estey & Wier, 2014), taking into account the capability of the GNSS receivers used in this study, considering only maintaining the GPS constellation as it is the common constellation in both receivers, avoiding biases in the position estimation, since there is a constellation difference. The static relative method was conditioned to Mexican CORS CULC at 15 s but the original sampling rate was configured at 5 hz due to the loss in observations in dual frequency low-cost GNSS receiver (Romero-Andrade et al., 2021). Similarly, all observations were decimated to 15 s with TEQC software for static relative method, therefore Topcon Tools (Topcon, 2009) software was used for processing observations. Code and Phase observables were used with an elevation cut off angle of 15° (10 to 15° is commonly used as less elevation in the atmospheric effect degrade the received signal, since the visibility of the satellite is lower) (Hofmann-Wellenhof et al., 2007; Zamora-Maciél et al., 2020), precise ephemeris (SP3) from IGS (Spofford & Remondi, 1994), and IGS ANTEX file for Receiver antenna phase center correction. The obtained coordinates were analyzed using the official reference frame in Mexico (ITRF08

at epoch 2010) (INEGI, 2016) in ENU system derived to which the coordinates of the CORS reference station are expressed in ITRF08 epoch 2010, considering the deformation of the geodetic frame over time due to the geodynamics present in Mexican territory (Romero-Andrade et al., 2021), to evaluate the changes in a topographic plane and not in the ellipsoidal model. Similarly, the results were evaluated according to the “Circle of Probable Error” (CEP) and “Vertical Positioning Accuracy” (EPV) (INEGI, 2010) at 95% of certainty in the positioning. Hence, a summary of the parameters used are given in Table 2.

Table 2: Summary of parameters used in Static relative method

| Parameters for static relative positioning |                             |
|--------------------------------------------|-----------------------------|
| Software                                   | Topcon Tools (Topcon, 2009) |
| Observable                                 | Code and Phase; L1 and L2   |
| Elevation cut off angle                    | 15°                         |
| Receiver antenna phase center correction   | IGS antex                   |
| Method                                     | Static relative             |
| Sampling rate                              | 5 hz                        |
| Occupation time                            | 2 h                         |
| Satellite orbits                           | Precise (IGS)               |
| Reference frame                            | ITRF08 epoch 2010.0         |

## 4 RESULTS

### 4.1 Relative positioning results

The reference coordinates derived from geodetic GNSS receivers that were used as a reference for the control are presented in the first part on Table 3. The second campaign was conducted similarly using geodetic GNSS receivers to evaluate the resulted coordinates from geodetic and low-cost GNSS receivers. For the reference coordinates, the achieved precision was in cm order, including the height component in long and short distance. The coordinates derived from geodetic order GNSS receiver were used as a reference for the ENU system.

Table 3: Reference and resulted coordinates for case A and B. First part is the reference values, second part is the resulted coordinates.

| Station name                                                     | Receiver | $\varphi$ (m)     | $\lambda$ (m)       | h(m)    | $\sigma_\varphi$ (m) | $\sigma_\lambda$ (m) | $\sigma_h$ (m) |
|------------------------------------------------------------------|----------|-------------------|---------------------|---------|----------------------|----------------------|----------------|
| <b>First part</b>                                                |          |                   |                     |         |                      |                      |                |
| <b>Geodetic coordinates taken as a reference for the case A.</b> |          |                   |                     |         |                      |                      |                |
| 1A                                                               |          | 24° 49' 37.77142" | 107° 22' 50.14687"  | 41.824  | 0.002                | 0.001                | 0.004          |
| 2A                                                               | ZENITH25 | 24° 49' 37.79275" | 107° 22' 49.911711" | 41.786  | 0.002                | 0.002                | 0.004          |
| 3A                                                               |          | 24° 49' 37.80356" | 107° 22' 49.80198"  | 41.789  | 0.002                | 0.001                | 0.004          |
| <b>Geodetic coordinates taken as a reference for the case B.</b> |          |                   |                     |         |                      |                      |                |
| A                                                                | ZENITH25 | 24° 48' 51.52890" | 107° 08' 56.20646"  | 127.827 | 0.003                | 0.001                | 0.002          |
| B                                                                |          | 24° 48' 51.71003" | 107° 08' 54.29876"  | 127.84  | 0.005                | 0.002                | 0.002          |

| Station name                            | Receiver                      | $\varphi$ (m)   | $\lambda$ (m)     | h(m)    | $\sigma_\varphi$ (m) | $\sigma_\lambda$ (m) | $\sigma_h$ (m) |
|-----------------------------------------|-------------------------------|-----------------|-------------------|---------|----------------------|----------------------|----------------|
| <b>Second part</b>                      |                               |                 |                   |         |                      |                      |                |
| <b>Obtained coordinates for case A.</b> |                               |                 |                   |         |                      |                      |                |
| 1A                                      | ZENITH25                      | 24°49'37.76861" | 107°22'50.15176"  | 41.777  | 0.002                | 0.001                | 0.004          |
|                                         | NEO-6T                        | 24°49'37.76891" | 107°22'50.17960"  | 41.983  | 0.002                | 0.002                | 0.004          |
|                                         | NEO-M8T                       | 24°49'37.77153" | 107°22'50.14728"  | 41.999  | 0.002                | 0.002                | 0.006          |
|                                         | ZED-F9P                       | 24°49'37.77148" | 107°22'50.14690"  | 42.040  | 0.002                | 0.002                | 0.006          |
| 2A                                      | ZENITH25                      | 24°49'37.79003" | 107°22'49.92204"  | 41.777  | 0.002                | 0.002                | 0.004          |
|                                         | NEO-6T                        | 24°49'37.79297" | 107°22'49.91718"  | 41.983  | 0.002                | 0.001                | 0.004          |
|                                         | NEO-M8T                       | 24°49'37.79281" | 107°22'49.911745" | 41.892  | 0.002                | 0.001                | 0.004          |
|                                         | ZED-F9P                       | 24°49'37.80339" | 107°22'49.90678"  | 43.172  | 0.196                | 0.145                | 0.263          |
| 3A                                      | ZENITH25                      | 24°49'37.80082" | 107°22'49.80670"  | 41.789  | 0.002                | 0.001                | 0.004          |
|                                         | NEO-6T                        | 24°49'37.80079  | 107°22'49.80662   | 41.999  | 0.002                | 0.002                | 0.004          |
|                                         | NEO-M8T                       | 24°49'37.80368" | 107°22'49.80189"  | 41.993  | 0.002                | 0.002                | 0.004          |
|                                         | ZED-F9P                       | 24°49'37.8034"  | 107°22'49.80181"  | 41.993  | 0.003                | 0.003                | 0.009          |
| <b>Obtained coordinates for case B.</b> |                               |                 |                   |         |                      |                      |                |
| A                                       | ZED-F9P<br>(ASTECH701975.01A) | 24°48'51.52889" | 107°08'56.20738"  | 127.909 | 0.007                | 0.005                | 0.019          |
| B                                       | ZED-F9P<br>(ASTECH701975.01A) | 24°48'51.71086" | 107°08'54.29955"  | 127.967 | 0.007                | 0.006                | 0.019          |

The obtained coordinates for the Cases A and B (Table 3), were precise in a mm order, nevertheless, the worst case was presented on dual frequency ZED-F9P low-cost receiver on point 2A. This is due to sensibility of the receiver to track weak signals (multipath effect), also the receiver lost observations at high frequencies (Romero-Andrade et al., 2021). For receivers NEO-6T and NEO-M8T, similar precisions were obtained with the height component at the worst precision. For the Case B, the obtained results were precise with a mm order for the horizontal component and cm order for vertical component. The obtained solutions presented in Table 4 and Figure 6 - 7 are precise in some cases. Considering the geodetic order receiver, the differences are in cm level for the Case A. The second worst obtained solutions are found for NEO-6T receiver. Finally, the receiver with the best performance is the ZED-F9P. Even if the low-cost receivers are used with a geodetic order antenna with IGS calibration, in some circumstances the multipath effect presented in the surrounding affects concededly the obtained solutions such as point 3A with ZED-F9P model.

Table 4: Differences between computed and reference coordinates expressed in Topocentric coordinates (ENU).

| Station name                            | Receiver | E (m) | N (m)  | U (m)  |
|-----------------------------------------|----------|-------|--------|--------|
| <b>Obtained coordinates for case A.</b> |          |       |        |        |
| 1A                                      | ZENITH25 | 0.012 | -0.007 | -0.045 |
|                                         | NEO-6T   | 0.796 | 0.623  | 0.161  |
|                                         | NEO-M8T  | 0.011 | 0.003  | 0.175  |
|                                         | ZED-F9P  | 0.001 | 0.001  | 0.216  |



| Station name                            | Receiver | E (m)  | N (m)  | U (m)  |
|-----------------------------------------|----------|--------|--------|--------|
| <b>2A</b>                               | ZENITH25 | 0.164  | -0.004 | -0.007 |
|                                         | NEO-6T   | 0.153  | 0.006  | 0.197  |
|                                         | NEO-M8T  | 0.001  | 0.001  | 0.196  |
|                                         | ZED-F9P  | -0.138 | 0.327  | 1.386  |
| <b>3A</b>                               | ZENITH25 | 0.007  | -0.005 | 0.002  |
|                                         | NEO-6T   | 0.005  | -0.006 | 0.212  |
|                                         | NEO-M8T  | -0.002 | -0.005 | 0.204  |
|                                         | ZED-F9P  | -0.004 | -0.004 | 0.250  |
| <b>Obtained coordinates for case B.</b> |          |        |        |        |
| <b>A</b>                                | ZENITH25 | 0.004  | 0.004  | -0.028 |
|                                         | ZED-F9P  | 0.010  | 0.014  | 0.218  |
| <b>B</b>                                | ZENITH25 | 0.005  | 0.008  | -0.036 |
|                                         | ZED-F9P  | -0.001 | 0.001  | 0.153  |

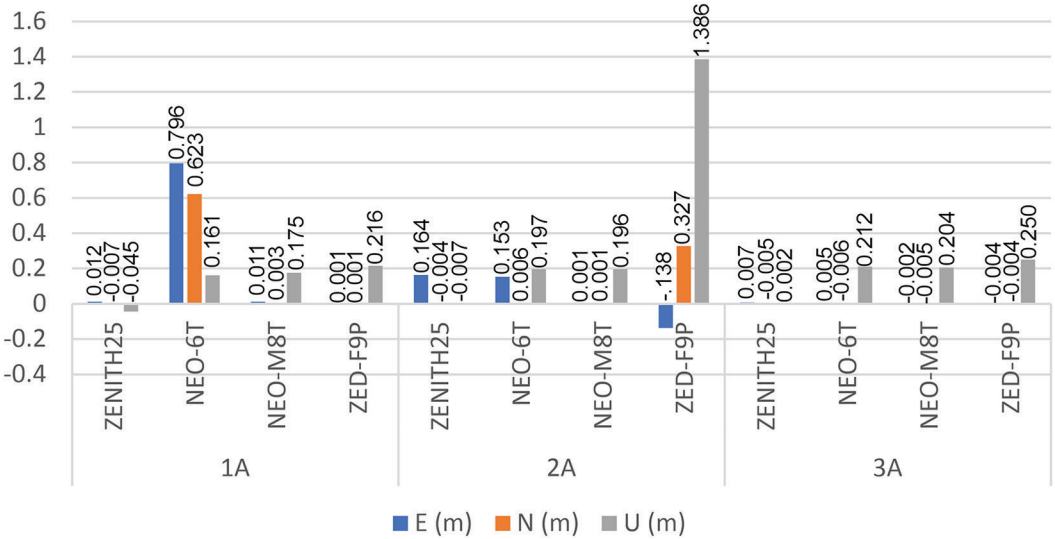


Figure 6: Differences between reference and computed coordinates expressed in Topocentric coordinates for case A.

For Case B which was performed to a long-distance (Figure 7), the best device was selected based on its performance which undoubtedly being ZED-F9P. The results show an accurate solution in a mm order for point B. In comparison with case A, the accuracy is maintained at short and long distances from the reference station. Nevertheless, for cases A and B, the vertical component reached cm level being the worst value.

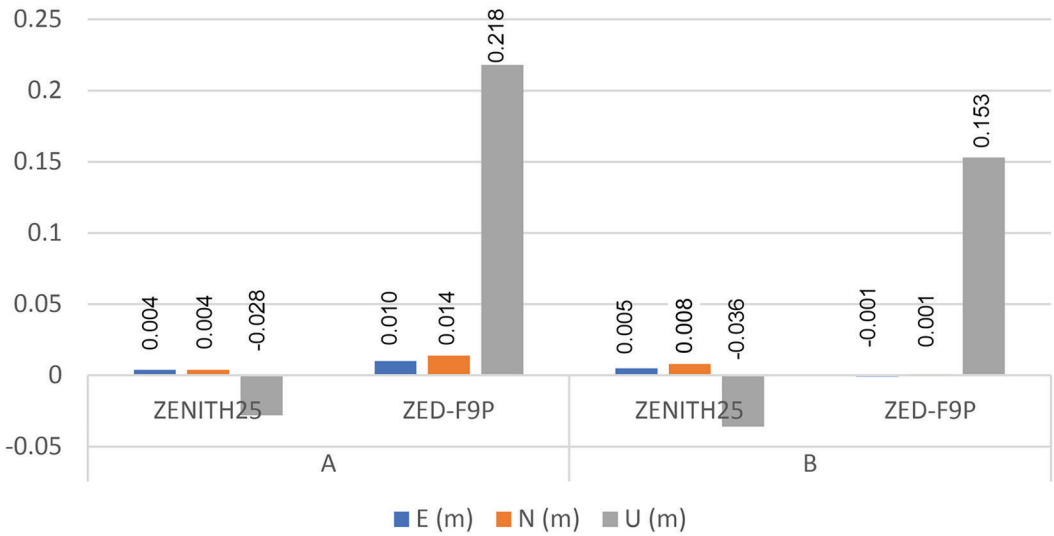


Figure 7: Differences between reference and computed coordinates expressed in Topocentric coordinates for case B.

### 3.2 Circle of probable error and Vertical Positioning Accuracy evaluation

The CEP and EPV evaluation including GGM10 model (for evaluate the vertical component according to the statements of INEGI) are presented in Table 5. For Case A, the standard deviation was in mm order as in some stations, though, only with ZED-F9P model from station 2 is in cm order due to the environment conditions. Similarly, the regulations of less than 5 cm are followed by CEP and EPV parameters. For the same receiver in station 2, the obtained values are in cm order. Some of the low-cost receivers obtain similar accuracy than a geodetic receiver with differences of mm. This indicates that it is possible to use the low-cost receivers if the regulations allow it. Regarding Case B, in both the stations similar performance were found with an mm order, nevertheless, the Up component is less precise than the geodetic order receiver, and this is seen in the CEP and EPV parameters.

Table 5: Circle of Probable Error and Vertical Positioning Accuracy Evaluation, including GGM10 model.

| Point         | Receiver | $\sigma_E$ (m) | $\sigma_N$ (m) | $\sigma_U$ (m) | CEP (m) | EPV(m) | GGM10(m) |
|---------------|----------|----------------|----------------|----------------|---------|--------|----------|
| <b>Case A</b> |          |                |                |                |         |        |          |
| 1A            | Geodetic | 0.001          | 0.002          | 0.004          | 0.004   | 0.008  | 0.392    |
|               | NEO-6T   | 0.002          | 0.002          | 0.004          | 0.005   | 0.008  | 0.392    |
|               | NEO-M8T  | 0.002          | 0.002          | 0.006          | 0.005   | 0.011  | 0.392    |
|               | ZED-F9P  | 0.005          | 0.002          | 0.006          | 0.005   | 0.012  | 0.392    |
| 2A            | Geodetic | 0.002          | 0.002          | 0.004          | 0.005   | 0.008  | 0.392    |
|               | NEO-6T   | 0.001          | 0.002          | 0.004          | 0.004   | 0.008  | 0.392    |
|               | NEO-M8T  | 0.001          | 0.002          | 0.004          | 0.004   | 0.008  | 0.392    |
|               | ZED-F9P  | 0.145          | 0.196          | 0.263          | 0.417   | 0.515  | 0.647    |
| 3A            | Geodetic | 0.001          | 0.002          | 0.004          | 0.004   | 0.008  | 0.392    |

| Point         | Receiver                  | $\sigma_E$ (m) | $\sigma_N$ (m) | $\sigma_U$ (m) | CEP (m) | EPV(m) | GGM10(m) |
|---------------|---------------------------|----------------|----------------|----------------|---------|--------|----------|
|               | NEO-6T                    | 0.002          | 0.002          | 0.004          | 0.005   | 0.008  | 0.392    |
|               | NEO-M8T                   | 0.002          | 0.002          | 0.004          | 0.005   | 0.008  | 0.392    |
|               | ZED-F9P                   | 0.003          | 0.003          | 0.009          | 0.008   | 0.018  | 0.392    |
| <b>Case B</b> |                           |                |                |                |         |        |          |
| A             | Geodetic                  | 0.002          | 0.003          | 0.002          | 0.007   | 0.004  | 0.392    |
|               | ZED-F9P<br>(ASH701975.01) | 0.005          | 0.006          | 0.019          | 0.013   | 0.037  | 0.392    |
| B             | Geodetic                  | 0.002          | 0.005          | 0.002          | 0.009   | 0.004  | 0.392    |
|               | ZED-F9P<br>(ASH701975.01) | 0.005          | 0.006          | 0.017          | 0.013   | 0.033  | 0.392    |

Regarding to the GGM10, the obtained values are greater than 5 cm (INEGI, 2010) derived from the precision of the 0.20 m. Nevertheless, the GGM10 model is the orthometric height reference used for the ITRF08 epoch 2010.0 in Mexico. Notwithstanding, this model is the reference surface of orthometric heights linked to ITRF08 epoch 2010.0 in Mexico, so this evaluation allows it to be considered for joint applications of low-cost GNSS receivers and the certainty obtained with the GGM10 model in those applications where it is permissible (not greater than 5 cm), as well as resource savings compared to leveling techniques. In the same way, if the GGM10 model is not considered for there was no certainty in levelling, all values agree with the reliability value only in the ellipsoidal height. On this sense, the height remains one of the main challenges not only for these low-cost GNSS equipment, but for the geoidal models themselves so it requires a more in-depth study for the vertical component.

**5 DISCUSSION**

The positioning obtained by using different receivers is precise, however, for the single frequency the accuracy tends to be more stable in comparison with the dual-frequency low-cost receivers such as ZED-FP9, as noted in the experiment. Regarding to the achieved accuracy, the solution that is obtained in Romero-Andrade et al. (2021) is more precise and similar to Alkan et al. (2015) even when Precise Point Positioning in urban areas are used that is less precise than static relative method, which is derived from the surrounding environment and the antenna location. Regarding the accuracy in real time techniques such as Real Time Kinematic (RTK), Garrido-Carretero et al. (2019) obtained precision in order of 2.5 mm and 4.5 mm for the horizontal and vertical component, respectively, being similar to our solution. However, this result is only seen in short distances, as for a long distance the obtained solution could reach almost to cm. On the other hand, as presented by Cutugno et al. (2020); Garrido-Carretero et al. (2019); Romero-Andrade et al. (2019, 2021, 2021 a); Zamora Maciel et al. (2020) the vertical component continues being the less precise reaching the cm.

**6 CONCLUSIONS**

According to the results obtained, the following statements can be concluded:

- The low-cost GNSS receivers presented high horizontal precision, even when a single frequency is used. Nevertheless, for Up component the dual frequency showed better performance. Similarly, a

cm difference was observed with the geodetic order receiver.

- The evaluation using static relative method showed a high precision when it was considered long distances between the reference station and low-cost receiver and 2 h of observations.
- The performance of the dual frequency low cost GNSS receivers are sensitive to the multipath effect, which directly impacts the positioning. However, the static relative method achieves a higher accuracy and precision.
- The use of the geodetic grade antenna in combination with low cost GNSS showed higher accuracy, nevertheless, the height component still being the less precise. In this sense, if GGM10 model from INEGI is used, the height reaches a cm level. On the other hand, the height component can be used without the inclusion of the GGM10 model.
- Based on the obtained results, the low-cost GNSS is recommendable to be used for geodetic and topography purposes according to the accuracy requirements that could be up to millimeter order. Although, the height component continues being the least accurate even if the geodetic grade antenna was used.
- In the same way, the NEO-6T receiver show the best performance in all cases even when single frequency is used.
- In the case of A, the single frequency low cost NEO-M8T showed a mm precision being a good performer even similar to the dual-frequency ZED-F9P, while on the other hand, the NEO-6T presents the worst precision.
- For the dual-frequency ZED-F9P receiver, the results are highly precise in most of the cases reaching mm level of precision. Similarly, for case B, the dual-frequency ZED-F9P receiver presents higher accuracy at long distances.

## Acknowledgements

The authors would also like to thank all anonymous reviewers for their valuable comments which refined the present work. Also, the authors are grateful to the students (Lizbeth Santiago, Fernanda Castelo, Donato Félix-Ortega and Rafaela M. Llanes-Hernández) who help to perform the observations for the experiment.

## Funding

This research was funded by CONACyT (Consejo Nacional de Ciencia y Tecnología) and Autonomous University of Sinaloa, Mexico, grand number CVU: 429125, 1142605. Also, this project was funded by PROFAPI 2022 with number PRO\_A1\_027.

## Literature and References

- Alkan, R. M., Ilçi, V., Ozulu, I. M., & Saka, M. H. (2015). A comparative study for accuracy assessment of PPP technique using GPS and GLONASS in urban areas. *Measurement: Journal of the International Measurement Confederation*, 69, 1–8. <https://doi.org/10.1016/j.measurement.2015.03.012>
- Cina, A., & Piras, M. (2015). Performance of low-cost GNSS receiver for landslides monitoring: test and results. *Geomatics, Natural Hazards and Risk*, 6(5–7), 497–514. <https://doi.org/10.1080/19475705.2014.889046>
- Cutugno, M., Robustelli, U., & Pugliano, G. (2020). Low-cost GNSS software receiver performance assessment. *Geosciences (Switzerland)*, 10(2). <https://doi.org/10.3390/geosciences10020079>
- Estey, L., & Wier, S. (2014). Teqc Tutorial: basics of Teqc use and Teqc products (Issue June).
- Ferhat, G., Malet, J.-P., & Ullrich, P. (2015). Evaluation of different processing strategies of Continuous GPS (CGPS) observations for landslide monitoring. *EGU General*
- Naccieli Bojorquez-Pacheco, Rosendo Romero-Andrade, Manuel Edwiges Trejo-Soto, Daniel Hernández-Andrade, Karan Nayak, Ana Isela Vidal-Vega, Anibal Israel Arana-Medina, Gopal Sharma, Luis Enrique Acosta-Gonzalez, Richard Serrano-Agila | OCENA DELOVANJA ENO IN DVOFREKVENČNIH NIZKOCENOVNIH SPREJE-MNIKOV GNSS V STATIČNEM RELATIVNEM NAČINU | PERFORMANCE EVALUATION OF SINGLE AND DOUBLE-FREQUENCY LOW-COST GNSS RECEIVERS IN STATIC RELATIVE MODE | 235-248 |

Assembly Conference Abstracts, 17, 10582.

Garrido-Carretero, M. S., de Lacy-Pérez de los Cobos, M. C., Borque-Arancón, M. J., Ruiz-Armenteros, A. M., Moreno-Guerrero, R., & Gil-Cruz, A. J. (2019). Low-cost GNSS receiver in RTK positioning under the standard ISO-17123-8: A feasible option in geomatics. *Measurement: Journal of the International Measurement Confederation*, 137, 168–178. <https://doi.org/10.1016/j.measurement.2019.01.045>

Hofmann-Wellenhof, B., Lichtenegger, H., & Collins, J. (2001). *Global Positioning System (Fifth)*. Springer-Verlag. <https://doi.org/10.1007/978-7091-6199-9>

Hofmann-Wellenhof, B., Lichtenegger, H., & Wasle, E. (2007). *GNSS--global navigation satellite systems: GPS, GLONASS, Galileo, and more*. Springer Science & Business Media.

INEGI. (2010). Norma técnica de Estándares de Exactitud Posicional. 1–12.

INEGI. (2016). Procesamiento de datos GPS considerando deformaciones del Marco Geodésico.

Janos, D., & Kuras, P. (2021). Evaluation of Low-Cost GNSS Receiver under Demanding Conditions in RTK Network Mode. *Sensors (Basel, Switzerland)*, 21. <https://doi.org/https://doi.org/10.3390/s21165552>

Krietemeyer, A., Van der Marel, H., Van de Giesen, N., & Ten Veldhuis, M.-C. (2022). A Field Calibration Solution to Achieve High-Grade-Level Performance for Low-Cost Dual-Frequency GNSS Receiver and Antennas. *Sensors (Basel, Switzerland)*, 22(2267). <https://doi.org/https://doi.org/10.3390/s22062267>

Läpädät, A. M., Tiberius, C. C. J. M., & Teunissen, P. J. G. (2021). Experimental evaluation of smartphone accelerometer and low-cost dual frequency gnss sensors for deformation monitoring. *Sensors*, 21(23). <https://doi.org/10.3390/s21237946>

Nischan, T. (2016). GFZRNX - RINEX GNSS Data Conversion and Manipulation Toolbox. <https://doi.org/https://doi.org/10.5880/GFZ.1.1.2016.002>

Psychas, D., Bruno, J., Massarweh, L., & Darugna, F. (2019). Towards sub-meter positioning using android raw GNSS measurements. *Proceedings of the 32nd International Technical Meeting of the Satellite Division of the Institute of Navigation, ION GNSS+ 2019, October*, 3917–3931. <https://doi.org/10.33012/2019.17077>

Puskas, C. M., Meertens, C. M., Phillips, D. A., Blume, F., Rost, M., & UNAVCO. (2019). Introduction to Anubis software for GNSS quality control in the GAGE Facility and NOTA. In UNAVCO. UNAVCO. [https://www.unavco.org/data/gps-gnss/derived-products/docs/Poster\\_2019\\_SAGE-GAGE\\_Workshop\\_Puskas\\_Introduction-to-Anubis-software-for-GNSS-quality-control-in-the-GAGE-Facility-and-NOTA.pdf](https://www.unavco.org/data/gps-gnss/derived-products/docs/Poster_2019_SAGE-GAGE_Workshop_Puskas_Introduction-to-Anubis-software-for-GNSS-quality-control-in-the-GAGE-Facility-and-NOTA.pdf)

Romero-andrade, R., Trejo-soto, M. E., Vega-ayala, A., Hernández-Andrade, D., Vázquez-Ontiveros, J. R., & Sharma, G. (2021). Positioning Evaluation of Single and Dual-Frequency Low-Cost GNSS Receivers Signals Using PPP and Static Relative Methods in Urban Areas. *Applied Sciences (Switzerland)*, 1–17. <https://doi.org/https://doi.org/10.3390/app112210642>

Romero-Andrade, R., Zamora-Maciél, A., Uriarte-Adrián, J. D. J., Pivot, F., & Trejo-Soto, M. E. (2019). Comparative analysis of precise point positioning processing technique with GPS low-cost in different technologies with academic software. *Measurement: Journal of the International Measurement Confederation*, 136. <https://doi.org/10.1016/j.measurement.2018.12.100>

Romero-Andrade, Rosendo, Cabanillas-zavala, J. L., Hernández-andrade, D., Trejo-soto, M. E., & Monjardin-armenta, S. A. (2020). Análisis Comparativo Del Posicionamiento GNSS Utilizando Receptor De Bajo Costo U-Blox De Doble Frecuencia Para Aplicaciones Topógrafo-Geodésicas. *European Scientific Journal*, 16(27), 289–312. <https://doi.org/10.19044/esj.2020.v16n27p289>

Romero-Andrade, Rosendo, Trejo-Soto, M. E., Vázquez-Ontiveros, J. R., Hernández-Andrade, D., & Cabanillas-Zavala, J. L. (2021). Sampling rate impact on Precise Point Positioning with a Low-Cost GNSS receiver. *Applied Sciences (Switzerland)*, 11(GNSS Techniques for Land and Structure Monitoring), 17. <https://doi.org/https://doi.org/10.3390/app11167669>

Romero-Andrade, Rosendo, Zamora-Maciél, A., Uriarte-Adrián, J. de J., Pivot, F., & Trejo-Soto, M. E. (2019). Comparative analysis of precise point positioning processing technique with GPS low-cost in different technologies with academic software. *Measurement*, 136, 337–344. <https://doi.org/10.1016/j.measurement.2018.12.100>

Skorupa, B. (2020). The problem of GNSS positioning with measurements recorded using Android mobile devices. *Budownictwo i Architektura*, 18(3), 051–062. <https://doi.org/10.35784/bud-arch.738>

Spofford, P. R., & Remondi, B. W. (1994). The national geodetic survey standard GPS format SP3. SP3-a Format) Available from the IGS Website: [http://igs.cbl.gov.nasa.gov/igs/Data/Format/Sp3\\_docu.Txt](http://igs.cbl.gov.nasa.gov/igs/Data/Format/Sp3_docu.Txt)

Takasu, T. (2013). RTKLIB 2.4.2 Manual (Issue C). [http://www.rtklib.com/prog/manual\\_2.4.2.pdf%0Ahttp://www.rtklib.com/rtklib.htm](http://www.rtklib.com/prog/manual_2.4.2.pdf%0Ahttp://www.rtklib.com/rtklib.htm)

Topcon. (2009). *Manual Reference Topcon Tools (p. 606)*. Topcon Tools Reference Manual.

Tsakiri, M., Sioulis, A., & Piniotis, G. (2018). The use of low-cost, single-frequency GNSS receivers in mapping surveys. *Survey Review*, 50(358), 46–56. <https://doi.org/10.1080/00396265.2016.1222344>

Tunini, L., Zuliani, D., & Magrin, A. (2022). Applicability of Cost-Effective GNSS sensor for crustal deformation studies. *Sensors (Basel, Switzerland)*.

Wielgocka, N., Hadas, T., Kaczmarek, A., & Marut, G. (2021). Feasibility of using low-cost dual-frequency gnss receivers for land surveying. *Sensors*, 21(6), 1–14. <https://doi.org/10.3390/s21061956>

Xiao, Y., Yao, M. H., Tang, S. H., Liu, H. F., Xing, P. W., & Zhang, Y. (2020). Data Quality Check and Visual Analysis of Cors Station Based on Anubis Software. *ISPRS - International Archives of the Photogrammetry, Remote Sensing and Spatial Information Sciences, XLII-3/W10(November 2019)*, 1295–1300. <https://doi.org/10.5194/isprs-archives-xlii-3-w10-1295-2020>

Zamora-Maciél, A., Romero-Andrade, R., Moraila-Valenzuela, C. R., & Pivot, F. (2020). Evaluación de receptores GPS de bajo costo de alta sensibilidad para trabajos geodésicos. Caso de estudio : línea base geodésica Evaluación de receptores GPS de bajo costo de alta sensibilidad para trabajos geodésicos. Caso de estudio : línea base geodé. *Ciencia Ergo-Sum*, 27, 0–17.





Bojorquez-Pacheco N., Romero-Andrade R., Trejo-Soto M.E., Hernández-Andrade D., Nayak K., Vidal-Vega A.I., Arana-Medina A.I., Sharma G., Acosta-Gonzalez L.E., Serrano-Agila R. (2023). Performance evaluation of single and double-frequency low-cost GNSS receivers in static relative mode. *Geodetski vestnik*, 67 (2), 235-248.

DOI: <https://doi.org/10.15292/geodetski-vestnik.2023.02.235-248>

**Ing. Naccieli Bojorquez-Pacheco**

Autonomous University of Sinaloa, Culiacán de Rosales,  
Sinaloa, México  
e-mail: [naccielibojorquez.facite@uas.edu.mx](mailto:naccielibojorquez.facite@uas.edu.mx)

**Dr. Rosendo Romero-Andrade**

Autonomous University of Sinaloa, Culiacán de Rosales,  
Sinaloa, México  
e-mail: [r.romero11@info.uas.edu.mx](mailto:r.romero11@info.uas.edu.mx)

**Dr. Manuel Edwiges Trejo-Soto**

Autonomous University of Sinaloa, Culiacán de Rosales,  
Sinaloa, México  
e-mail: [mtrejosoto@uas.edu.mx](mailto:mtrejosoto@uas.edu.mx)

**Ing. Daniel Hernández-Andrade**

Autonomous University of Sinaloa, Culiacán de Rosales,  
Sinaloa, México  
e-mail: [danielhernandez.facite@uas.edu.mx](mailto:danielhernandez.facite@uas.edu.mx)

**Msc. Karan Nayak**

Autonomous University of Sinaloa, Culiacán de Rosales,  
Sinaloa, México  
e-mail: [nayakkaran.facite@uas.edu.mx](mailto:nayakkaran.facite@uas.edu.mx)

**Msc. Ana Isela Vidal-Vega**

Autonomous University of Sinaloa, Culiacán de Rosales,  
Sinaloa, México  
e-mail: [anavidal@uas.edu.mx](mailto:anavidal@uas.edu.mx)

**Msc. Aníbal Israel Arana-Medina**

Autonomous University of Sinaloa, Culiacán de Rosales,  
Sinaloa, México  
e-mail: [anibal.arana@uas.edu.mx](mailto:anibal.arana@uas.edu.mx)

**Dr. Gopal Sharma**

North Eastern Space Applications Centre, Umiam, 793103,  
Meghalaya, India  
e-mail: [gops.geo@gmail.com](mailto:gops.geo@gmail.com)

**Dr. Luis Enrique Acosta-Gonzalez**

Center for CAD/CAM Studies,  
Faculty of Engineering, University of Holguín,  
Cuba, 4 XX Aniversario Avenue, Piedra Blanca neighborhood  
e-mail: [luis.acosta.glez@gmail.com](mailto:luis.acosta.glez@gmail.com)

**Dr. Richard Serrano-Agila**

Department of Geoscience,  
Universidad Técnica Particular de Loja  
San Cayetano Alto. PO 11-01-608, Ecuador  
e-mail: [rgserrano@utpl.edu.ec](mailto:rgserrano@utpl.edu.ec)